

RESEARCH

Open Access



# Geochemical studies of carbonates of the Tayiba Formation (Upper Eocene), Abu Zenima area, West Central Sinai

Esmat A. Abou El-Anwar

## Abstract

**Background:** Tayiba Formation situated at the entrance of Wadi El-Tayiba. It unconformably overlies the Late Eocene Tanka Formation and unconformably underlies the Early Miocene Nukhul Formation. Severely authors studied this formation geologically, stratigraphically, and petrographically. But, geochemical studies on the rare earth elements to illustrate the depositional environments are seldom.

**Results:** Results were revealed that, mineralogically, the carbonate rocks in the Tayiba Formation are mainly composed of calcite, dolomite, quartz and clay minerals. The terminal parts of the studied Tayiba Formation are more dolomitized relative to the middle beds.

Geochemical analysis revealed that the carbonates of Tayiba Formation were deposited under shallow, oxidizing, marine environment. The dolomitization process has taken place in marine environment. Carbonate rocks of the Tayiba Formation are highly enriched in trace elements and highly to moderately rare earth elements. The studied carbonate rocks characterized by light REE (LREE) enrichment than heavy REE (HREE).

**Conclusions:** The redox-sensitive and rare earth elements study indicates that the carbonate rocks in the Tayiba Formation were deposited under anoxic to oxic marine environment. Also, the trace and rare earth elements values indicated that the studied carbonate rocks are mainly hydrogenous sources. These elements may be derived from more mafic sources.

**Keywords:** Abu Zenima, Tayiba Formation, Geochemistry, Rare earth elements

## Introduction

Tayiba Formation has a considerable importance to the history of the opening of the Red Sea and the Gulf of Suez. This formation represented a transitional stage between the pre-rifting Eocene marine sediments and the Early Miocene transgression of the newly formed rift (Refaat and Imam 1999).

Lithostratigraphically, the exposed Eocene successions in the south-western part of Sinai are mainly carbonate. The Eocene succession thickness recorded at Wadi Tayiba is about 152 m (Ibrahim et al. 2016).

Tayiba Formation is located at the mouth of Wadi El-Tayiba. It unconformably overlies the Late Eocene Tanka Formation (interbedded chalky limestone and

shale with argillaceous limestone) and unconformably underlies the Early Miocene Nukhul Formation. This is significant with polymictic conglomerate beds characteristic of the unconformable surfaces (El Barkooky and El-Araby 1999). Also, they mentioned which conformable up change from shallow marine carbonates (Tanka Formation) to tidally influenced shallow marine clastics and carbonates (Tayiba Formation) indicate a swallowing of water depth during the Late Oligocene. Jackson et al. (2006) revealed that the Tayiba Formation represented slight changes in relative sea level. In addition, Van Wagoner et al. (1988) mentioned that the eustatically or tectonically driven sea-level drop leads to the pre-rift/syn-rift contact unconformity. Refaat and Imam (1999) mentioned that at Wadi El-Tayiba, the Tayiba Formation is composed of marine, yellow red siltstone and mudstone, alternating with reddish-yellow and grayish argillaceous to sandy

Correspondence: [abouelanwar2004@yahoo.com](mailto:abouelanwar2004@yahoo.com)

Geological Sciences Department, National Research Center, 33 El Bohouth St. (former El Tahrir St.)- Dokki, POB: 12622, Giza, Egypt

limestone, highly fossiliferous with reworked Nummulites spp. and molluscan shell fragments.

**Materials and methods**

Fifteen representative samples were collected from the carbonate rocks of Abu Zenima, Tayiba Formation in West Central Sinai. Mineralogically, three selected samples were investigated by the X-ray technique at the Egyptian Mineral Resources Authority (Dokki, Egypt) using a PAN analytical X-Ray Diffraction equipment model X'Pert PRO with Secondary Monochromator; Cu-radiation ( $\lambda = 1.542 \text{ \AA}$ ) at 45 K.V., 35 M.A., and

scanning speed  $0.02^\circ/\text{s}$  were used. The diffraction charts and relative intensities are compared with ICDD files. Eight samples were selected to determine the chemical composition by using Axios Sequential WD\_XRF Spectrometer, Analytical 2005 in the National Research Center laboratories. ASTM E 1621 standard guide for elemental analysis by wavelength dispersive X-Ray Fluorescence Spectrometer, and ASTM D 7348 standard test methods for loss of ignition (LOI) of solid combustion. The fabric and the size of the synthesized samples were characterized via SEM coupled with energy-dispersive spectroscopy EDAX (SEM Model Quanta FEG 250),

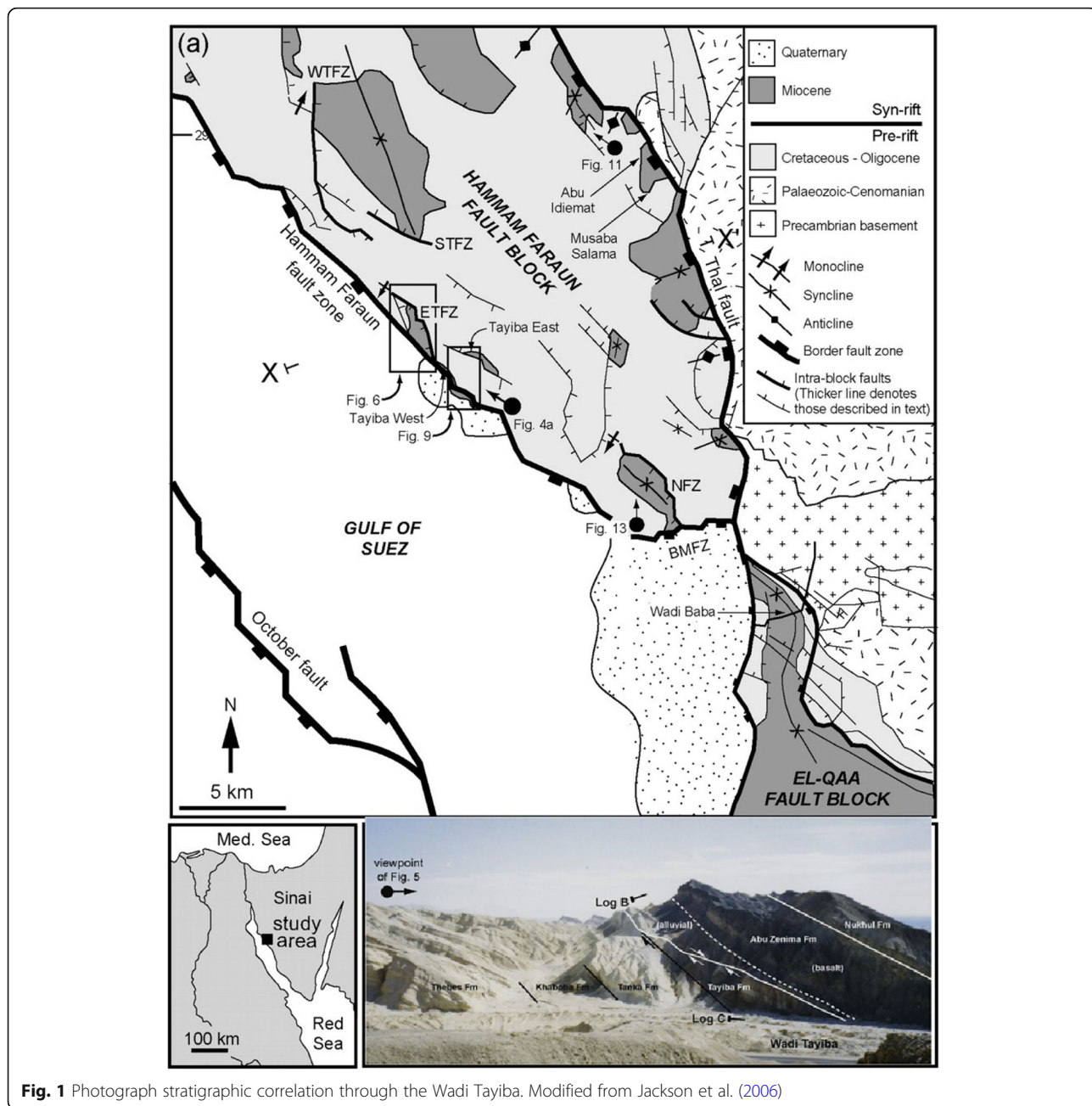
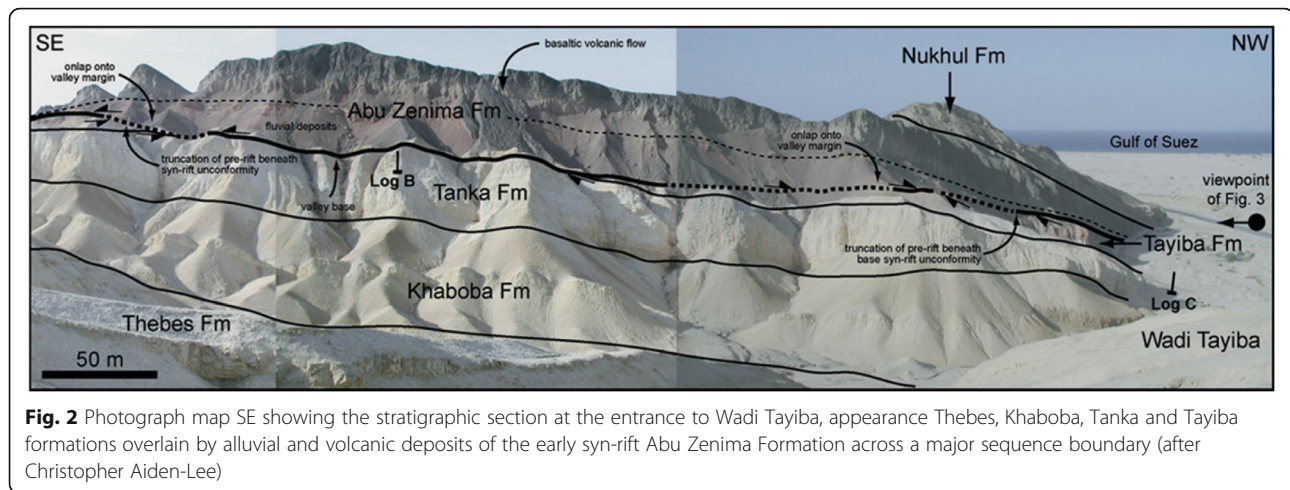


**Fig. 1** Photograph stratigraphic correlation through the Wadi Tayiba. Modified from Jackson et al. (2006)



carried out in the National Research Center laboratories. The samples were selected based on their hand specimen description to represent the formation for chemical and mineralogical studies.

### Geologic setting

Abu Zenima area is located on the eastern part of the Gulf of Suez, west-central Sinai (Fig. 1). The stratigraphical sequence ranges in age from late Cretaceous to middle Miocene. In Abu Zenima area, the Tayiba Red Beds (Hume et al. 1920) or Tayiba Formation (Youssef and Abdel Malik 1969) consists generally of red shale and sandstone with polymictic conglomerate and subordinate argillaceous to sandy limestone beds. Two major unconformity surfaces are represented with obvious basal polymictic conglomerate beds. This formation was underlying the Middle Eocene Tanka Formation and overlying the Early Miocene Abu Zenima Formation. Wadi Tayiba is located about 2 km north of the village of Abu Zenima.

All previous studies indicate that the oldest pre-rift unit in the Wadi Tayiba is the Upper Eocene Tanka Formation, which consists of micritic, pelletaloid limestones, containing a range of shallow water benthic foraminifera (e.g., *Quingelocina* sp.) According to the faunal assemblage, the Tanka Formation was deposited on a carbonate platform in an upper shelf environment (Abul-Nasr and Thunell 1987).

Late pre-rift marine carbonates, mudstones and sandstones of the Thebes, Khaboba, Tanka and Tayiba formations are erosively overlain by alluvial and volcanic deposits of the early syn-rift Abu Zenima Formation transversely a major sequence boundary (Jackson et al. 2006) (Fig. 2).

The aim of the present work is to study the mineral and chemical composition of the carbonate rocks of the Tayiba Formation (Upper Eocene) in Abu Zenima area to reveal their depositional environments and if there is a possibility of utilizing them in some purposes.

### Results

Chemically, the studied samples composed mainly of CaO (26.39%), SiO<sub>2</sub> (25.93%), Al<sub>2</sub>O<sub>3</sub> (10.67%), Fe<sub>2</sub>O<sub>3</sub> (3.13%), MgO (1.88%), and Na<sub>2</sub>O (1.26%). Mineralogically, the studied carbonate rocks at Tayiba Formation, Upper Eocene, Abu Zenima area, are consisting of calcite and dolomite as well as clay minerals. Dolomitization was the main diagenetic features encountered in the carbonate rocks of Tayiba Formation. Table 1 shows the chemical analysis data for major, trace, and rare earth elements of the studied carbonate rocks and the relation between them quoted in Table 2.

### Discussion

#### Mineralogy

X-ray diffraction XRD analyses were carried out on some selected samples. X-ray patterns revealed that the dominating minerals in the studied samples are mainly dolomite and calcite, quartz in addition to clay minerals.

#### Geochemistry

##### Major elements

Chemical analysis data of major, trace, and rare earth elements are quoted in Table 1. The normative dolomite content of the studied samples ranges from 4.3 to 11.44%, averaging 8.61%. Calcite precipitated from seawater would contain from 5.9 to 27.1% MgCO<sub>3</sub> by weight, while calcite exposed to meteoric water diagenesis will lose most of its magnesium content (Moore, 1989 and Morse and Mackenzie, 1990). The studied carbonate rocks contain up to 8.67% MgCO<sub>3</sub> and 6.52%, in average. This value revealed that the studied calcite was subjected to progressive diagenesis. MgO content varies from 0.94 to 2.5%. The terminal parts of the studied Tayiba Formation are more dolomitized relative to the middle beds. Though, it seems more eligible that the dolomitization process is controlled by the fracture and

**Table 1** Concentration of major (%), trace, and rare earth elements (ppm) of the studied carbonate rocks as well as ratios

| Element                        | 1     | 2     | 3     | 4     | 5     | 6     | 7     | 8     | Min.  | Max.  | Average |
|--------------------------------|-------|-------|-------|-------|-------|-------|-------|-------|-------|-------|---------|
| CaO                            | 26.62 | 25.73 | 27.1  | 25.94 | 27.54 | 25.41 | 24.95 | 27.8  | 24.95 | 27.8  | 26.39   |
| MgO                            | 1.77  | 1.81  | 1.54  | 0.94  | 1.99  | 2.1   | 2.4   | 2.5   | 0.94  | 2.5   | 1.88    |
| SiO <sub>2</sub>               | 26.75 | 26.63 | 25.31 | 27.37 | 25.14 | 24.7  | 26.4  | 25.1  | 24.7  | 27.37 | 25.93   |
| Al <sub>2</sub> O <sub>3</sub> | 10.2  | 10.15 | 10.54 | 10.94 | 12.15 | 9.85  | 11.2  | 10.34 | 9.85  | 12.15 | 10.67   |
| Fe <sub>2</sub> O <sub>3</sub> | 3.39  | 3.45  | 2.97  | 3.54  | 2.15  | 3.41  | 3.2   | 2.94  | 2.15  | 3.54  | 3.13    |
| Na <sub>2</sub> O              | 0.26  | 2.58  | 1.37  | 0.94  | 1.04  | 0.27  | 1.94  | 1.64  | 0.26  | 2.58  | 1.26    |
| K <sub>2</sub> O               | 0.71  | 0.62  | 0.82  | 0.74  | 0.51  | 0.75  | 0.84  | 0.56  | 0.51  | 0.84  | 0.69    |
| P <sub>2</sub> O <sub>5</sub>  | 0.37  | 0.37  | 0.36  | 0.35  | 0.41  | 0.41  | 0.52  | 0.31  | 0.31  | 0.52  | 0.39    |
| TiO <sub>2</sub>               | 0.68  | 0.67  | 0.65  | 0.61  | 0.75  | 0.81  | 0.75  | 0.67  | 0.61  | 0.81  | 0.70    |
| SrO                            | 0.115 | 0.114 | 0.12  | 0.12  | 0.18  | 0.13  | 0.12  | 0.14  | 0.114 | 0.18  | 0.13    |
| SO <sub>3</sub>                | 0.67  | 0.74  | 0.69  | 0.79  | 0.54  | 0.84  | 0.65  | 0.85  | 0.54  | 0.85  | 0.72    |
| Cl                             | 0.11  | 0.12  | 0.1   | 0.11  | 0.17  | 0.16  | 0.18  | 0.18  | 0.1   | 0.18  | 0.14    |
| LOI                            | 28.2  | 26.91 | 17.92 | 27.01 | 27.41 | 31.12 | 26.82 | 26.93 | 17.92 | 31.12 | 26.54   |
| Norm. Dolom.                   | 8.1   | 8.28  | 7.04  | 4.3   | 9.1   | 9.61  | 10.98 | 11.44 | 4.3   | 11.44 | 8.61    |
| V                              | 53.4  | 60    | 80    | 80.1  | 95    | 92    | 97    | 100   | 53.4  | 100   | 82.19   |
| Cr                             | 59.6  | 50.3  | 60.4  | 40.6  | 71.2  | 75    | 78    | 80    | 40.6  | 80    | 64.39   |
| Mn                             | 238.8 | 250.1 | 325.4 | 280.1 | 310   | 315   | 340   | 384   | 238.8 | 384   | 305.43  |
| Co                             | 5.6   | 6.7   | 5.8   | 7.1   | 8.4   | 6.8   | 7.9   | 8.9   | 5.6   | 8.9   | 7.15    |
| Ni                             | 47.2  | 50.3  | 61.4  | 62.8  | 71.52 | 68    | 79    | 90    | 47.2  | 90    | 66.28   |
| Cu                             | 10.1  | 10.5  | 12.4  | 15.3  | 16.4  | 15.2  | 17.3  | 17.9  | 10.1  | 17.9  | 14.39   |
| Zn                             | 109.1 | 120   | 112.8 | 151.2 | 165   | 105   | 164   | 134   | 105   | 165   | 132.64  |
| Mo                             | 3.5   | 4.2   | 5.7   | 5.9   | 6.2   | 4.8   | 6.4   | 7.9   | 3.5   | 7.9   | 5.58    |
| Zr                             | 129.4 | 135.1 | 140.8 | 159   | 145   | 159   | 164   | 179   | 129.4 | 179   | 151.41  |
| Pb                             | 7.6   | 8.6   | 9.1   | 10.1  | 12    | 11.4  | 12.9  | 16.1  | 7.6   | 16.1  | 10.98   |
| Rb                             | 19    | 20    | 25    | 30    | 24    | 26    | 29    | 32    | 19    | 32    | 25.63   |
| Ga                             | 11.4  | 12.5  | 14.3  | 12.3  | 13.7  | 13.2  | 14.2  | 15.4  | 11.4  | 15.4  | 13.38   |
| Se                             | 2     | 3     | 3     | 4     | 5     | 3     | 4     | 6     | 2     | 6     | 3.75    |
| Br                             | 2.5   | 3     | 4     | 5.5   | 5.4   | 3.1   | 4.7   | 4.5   | 2.5   | 5.5   | 4.09    |
| Y                              | 19.1  | 20.2  | 19.8  | 24.3  | 27.4  | 20.4  | 24.1  | 28.5  | 19.1  | 28.5  | 22.98   |
| Nb                             | 13.7  | 15.4  | 16.2  | 14.8  | 17.2  | 18.7  | 15.4  | 16.4  | 13.7  | 18.7  | 15.98   |
| As                             | 3.9   | 4.5   | 6.2   | 4.8   | 7.1   | 5.4   | 4.7   | 7.5   | 3.9   | 7.5   | 5.51    |
| Te                             | 2.1   | 2.5   | 2.3   | 3.7   | 3.9   | 3.1   | 4.2   | 3.8   | 2.1   | 4.2   | 3.20    |
| Sb                             | 4.1   | 4.5   | 5.1   | 4.8   | 5.7   | 2.5   | 3.1   | 3.8   | 2.5   | 5.7   | 4.20    |
| I                              | 23    | 25    | 27    | 29    | 30    | 29    | 25    | 34    | 23    | 34    | 27.75   |
| Cs                             | 7     | 8     | 6     | 9     | 8     | 8     | 7     | 8     | 6     | 9     | 7.63    |
| Ba                             | 162.7 | 170.5 | 180.3 | 185   | 190   | 189   | 172   | 201   | 162.7 | 201   | 181.31  |
| La                             | 27.4  | 28.5  | 29    | 30    | 35    | 37    | 25    | 40    | 25    | 40    | 31.49   |
| Nd                             | 13.1  | 15.2  | 12.4  | 13.9  | 16.7  | 14.8  | 15.1  | 17.2  | 12.4  | 17.2  | 14.80   |
| Sm                             | 17.4  | 18.4  | 20.3  | 19.7  | 21.8  | 19.9  | 20.2  | 22.7  | 17.4  | 22.7  | 20.05   |
| Hf                             | 0.3   | 0.4   | 0.3   | 0.5   | 0.6   | 0.4   | 0.5   | 0.6   | 0.3   | 0.6   | 0.45    |
| Sc                             | 24    | 22    | 27    | 26    | 27    | 31    | 32    | 35    | 22    | 35    | 28.00   |
| W                              | 15.8  | 16.8  | 17.6  | 17.9  | 18.4  | 18.1  | 14.9  | 19.2  | 14.9  | 19.2  | 17.34   |
| Ti                             | 2     | 2     | 3     | 2     | 2     | 2     | 3     | 3     | 2     | 3     | 2.38    |
| Ce                             | 15    | 18    | 19    | 22    | 25    | 26    | 25    | 27    | 15    | 27    | 22.13   |

**Table 1** Concentration of major (%), trace, and rare earth elements (ppm) of the studied carbonate rocks as well as ratios (Continued)

| Element  | 1      | 2      | 3      | 4      | 5      | 6      | 7      | 8      | Min.  | Max.  | Average |
|----------|--------|--------|--------|--------|--------|--------|--------|--------|-------|-------|---------|
| U        | 1.1    | 1.3    | 1.7    | 2.1    | 2.3    | 2.1    | 2.4    | 3.4    | 1.1   | 3.4   | 2.05    |
| Th       | 8.6    | 7.9    | 9.3    | 10.2   | 10.4   | 9.4    | 8.4    | 10.8   | 7.9   | 10.8  | 9.38    |
| Ta       | 4      | 3      | 2      | 4      | 4      | 3      | 4      | 4      | 2     | 4     | 3.50    |
| U/Mo     | 0.31   | 0.31   | 0.3    | 0.36   | 0.37   | 0.44   | 0.38   | 0.43   | 0.31  | 0.43  | 0.37    |
| V/Mo     | 15.26  | 14.29  | 14.04  | 13.58  | 15.32  | 19.17  | 15.16  | 12.66  | 15.26 | 12.66 | 14.74   |
| V/(V+Cr) | 0.47   | 0.54   | 0.57   | 0.66   | 0.57   | 0.55   | 0.55   | 0.56   | 0.57  | 0.56  | 0.60    |
| ΣLREEs   | 84.30  | 92.60  | 95.00  | 97.90  | 112.20 | 110.90 | 99.50  | 122.30 | 84.3  | 122.3 | 101.84  |
| ΣHREEs   | 43.10  | 42.20  | 46.80  | 50.30  | 54.40  | 51.40  | 56.10  | 63.50  | 42.2  | 63.5  | 50.98   |
| ΣREEs    | 366.50 | 390.40 | 412.80 | 429.20 | 459.90 | 444.60 | 414.10 | 493.60 | 366.5 | 493.6 | 426.39  |
| La/Ce    | 1.83   | 1.58   | 1.53   | 1.36   | 1.40   | 1.42   | 1.00   | 1.48   | 1.67  | 1.48  | 1.42    |

joint systems in the area, which maintain access to the dolomitizing fluids. Consequently, the dolomitization process was controlled by the fracture and joint in the area, which preserve access to the dolomitizing fluids. This result agrees with X-ray results.

SiO<sub>2</sub> content in the studied samples ranges from 24.7 to 27.37% with an average of 25.93%. Al<sub>2</sub>O<sub>3</sub> content ranges from 9.85 to 12.15% with an average 10.67% (Table 1). The carbonate rocks of the studied succession record average 1.26 and 0.69%, respectively of Na<sub>2</sub>O and K<sub>2</sub>O. The positive relation between SiO<sub>2</sub> and both Al<sub>2</sub>O<sub>3</sub> and K<sub>2</sub>O (Table 2) can mainly be attributed to the clay content, which is detected by X-ray diffraction analysis. The Eocene marine basin of deposition was relatively alkaline, close to the landmass that supplied the basin of deposition by quartz and clays (Ibrahim et al. 2016).

Fe<sub>2</sub>O<sub>3</sub> content of the studied carbonate sediments ranges from 2.15 to 3.54%, averaging 3.13%. The values for the Tayiba dolomite indicate the formation of dolomite in the near-surface oxidizing environment (Choquette and James, 1990, Loukina and Abou El-Anwar 1994 and Abou El-Anwar 2006 and Abou El-Anwar 2011). The positive correlation between Fe<sub>2</sub>O<sub>3</sub> and SiO<sub>2</sub> ( $r = 0.56$ ), suggests that iron is not completely associated with the terrigenous admixture but is rather a pigment. Also, the strong negative correlation between Fe<sub>2</sub>O<sub>3</sub> and Sr ( $r = -0.90$ ) indicates that there is no essential function of many microbes (Abou El-Anwar 2005, 2011, 2014 and Abou El-Anwar 2018a and Abou El-Anwar et al. 2017 and Abou El-Anwar 2018a, 2018b).

The strontium content of the studied carbonate rocks in the studied samples ranges from 964 to 1522 ppm, averaging 1099 ppm, which indicate late diagenetic resulting of dolomitization process (Veizer, et al., 1978 and Tucker and Wright 1990). The positive correlation between Sr and Ca ( $r = 0.56$ ) signified that calcite is still the main host of strontium in the studied carbonates (Table 2). The values of Sr content can be attributed to the long diagenetic history particularly the dolomitization stages. This

agrees with the findings of Brand and Veizer (1980) and Abou El-Anwar (2005 and 2006).

The average Sr content suggests that the dolomitization process has taken place in marine environment (Brand and Veizer 1980 and Abou El-Anwar 2011). The strong negative correlation between Sr and Na ( $r = -0.15$ ) indicates that Na does not couple with Sr during dolomitization. This is in disagreement with Moore and Chowdhury (1988), Loukina, et al., (2001), and Abou El-Anwar (2005 and 2006).

#### Trace and rare earth elements

Geochemical tools are used to identify and construe the parameters of normal environmental and origin. Thus, trace and REE elements are the most geochemical parameters that can be used to illustrate the paleo-climatic environments (Veizer and Mackenzie 2014 and Kamber, et al., 2014).

Carbonate rocks in the Tayiba Formation, Abu Zenima region, are highly enriched in trace elements (Zn = 132.6, Ni = 66.3, I = 27.8, and Mo = 5.1, ppm, Table 1 and Fig. 3) and highly to moderately rare earth elements (La = 31.5, Sc = 28, Y = 23, Sm = 20.1, W = 17.3, Nb = 16, Cs = 7.6, As = 5.5, Sb = 4.2, and Ta = 3.5 ppm, Fig. 4) compared with those of the UCC (Rudnick and Gao 2003).

The strong and moderate positive correlations between Al<sub>2</sub>O<sub>3</sub> and all immobile elements of trace and rare earth elements (Table 2) reveal that these elements are concentrated during weathering processes (Fedo et al. 1996). Almost all the trace and rare earth elements show positive relation with each other in the study carbonate rocks. Thus, these elements may be associated with each other or with the heavy minerals rather than with dolomite and clay minerals (Abou El-Anwar 2018b).

The radioactivity elements in the studied carbonate rocks are ranging from 1.1 to 3.4 with average 2.05 ppm for U and from 7.9 to 10.8 ppm for Th. Therefore, these contents are less than the allowed limits for radioactivity

**Table 2** Correlation matrix between the studied elements

|                                | CaO   | MgO   | SiO <sub>2</sub> | Al <sub>2</sub> O <sub>3</sub> | Fe <sub>2</sub> O <sub>3</sub> | Na <sub>2</sub> O | K <sub>2</sub> O | P <sub>2</sub> O <sub>5</sub> | TiO <sub>2</sub> | SrO   | SO <sub>3</sub> | Cl    | LOI   | Norm.D. | V     | Cr    | Mn    | Co    | Ni    | Cu    | Zn    | Mo   | Zr    |
|--------------------------------|-------|-------|------------------|--------------------------------|--------------------------------|-------------------|------------------|-------------------------------|------------------|-------|-----------------|-------|-------|---------|-------|-------|-------|-------|-------|-------|-------|------|-------|
| CaO                            | 1.00  |       |                  |                                |                                |                   |                  |                               |                  |       |                 |       |       |         |       |       |       |       |       |       |       |      |       |
| MgO                            | 0.07  | 1.00  |                  |                                |                                |                   |                  |                               |                  |       |                 |       |       |         |       |       |       |       |       |       |       |      |       |
| SiO <sub>2</sub>               | -0.41 | -0.56 | 1.00             |                                |                                |                   |                  |                               |                  |       |                 |       |       |         |       |       |       |       |       |       |       |      |       |
| Al <sub>2</sub> O <sub>3</sub> | 0.24  | -0.03 | 0.02             | 1.00                           |                                |                   |                  |                               |                  |       |                 |       |       |         |       |       |       |       |       |       |       |      |       |
| Fe <sub>2</sub> O <sub>3</sub> | -0.67 | -0.32 | 0.56             | -0.74                          | 1.00                           |                   |                  |                               |                  |       |                 |       |       |         |       |       |       |       |       |       |       |      |       |
| Na <sub>2</sub> O              | -0.10 | 0.23  | 0.18             | 0.10                           | -0.03                          | 1.00              |                  |                               |                  |       |                 |       |       |         |       |       |       |       |       |       |       |      |       |
| K <sub>2</sub> O               | -0.63 | -0.23 | 0.25             | -0.27                          | 0.56                           | -0.12             | 1.00             |                               |                  |       |                 |       |       |         |       |       |       |       |       |       |       |      |       |
| P <sub>2</sub> O <sub>5</sub>  | -0.64 | 0.35  | 0.04             | 0.37                           | -0.06                          | 0.10              | 0.43             | 1.00                          |                  |       |                 |       |       |         |       |       |       |       |       |       |       |      |       |
| TiO <sub>2</sub>               | -0.30 | 0.63  | -0.59            | 0.08                           | -0.25                          | -0.26             | 0.00             | 0.64                          | 1.00             |       |                 |       |       |         |       |       |       |       |       |       |       |      |       |
| SrO                            | 0.57  | 0.29  | -0.56            | 0.70                           | -0.90                          | -0.15             | -0.69            | 0.02                          | 0.39             | 1.00  |                 |       |       |         |       |       |       |       |       |       |       |      |       |
| SO <sub>3</sub>                | -0.15 | 0.00  | -0.07            | -0.75                          | 0.62                           | -0.05             | 0.11             | -0.48                         | -0.16            | -0.43 | 1.00            |       |       |         |       |       |       |       |       |       |       |      |       |
| Cl                             | 0.02  | 0.83  | -0.51            | 0.32                           | -0.45                          | 0.13              | -0.32            | 0.43                          | 0.66             | 0.56  | -0.02           | 1.00  |       |         |       |       |       |       |       |       |       |      |       |
| LOI                            | -0.35 | 0.29  | 0.04             | -0.11                          | 0.21                           | -0.32             | -0.31            | 0.19                          | 0.52             | 0.16  | 0.23            | 0.46  | 1.00  |         |       |       |       |       |       |       |       |      |       |
| Norm.D.                        | 0.07  | 1.00  | -0.56            | -0.03                          | -0.32                          | 0.22              | -0.23            | 0.35                          | 0.63             | 0.29  | 0.00            | 0.83  | 0.29  | 1.00    |       |       |       |       |       |       |       |      |       |
| V                              | 0.13  | 0.49  | -0.59            | 0.42                           | -0.49                          | 0.04              | -0.08            | 0.28                          | 0.43             | 0.56  | 0.08            | 0.80  | 0.06  | 0.49    | 1.00  |       |       |       |       |       |       |      |       |
| Cr                             | 0.16  | 0.92  | -0.73            | 0.10                           | -0.46                          | -0.04             | -0.12            | 0.38                          | 0.71             | 0.43  | -0.04           | 0.85  | 0.20  | 0.92    | 0.69  | 1.00  |       |       |       |       |       |      |       |
| Mn                             | 0.30  | 0.59  | -0.63            | 0.17                           | -0.41                          | 0.17              | -0.04            | 0.06                          | 0.23             | 0.35  | 0.23            | 0.69  | -0.18 | 0.59    | 0.89  | 0.73  | 1.00  |       |       |       |       |      |       |
| Co                             | 0.25  | 0.55  | -0.31            | 0.50                           | -0.52                          | 0.31              | -0.55            | 0.11                          | 0.23             | 0.64  | 0.02            | 0.85  | 0.30  | 0.55    | 0.78  | 0.54  | 0.68  | 1.00  |       |       |       |      |       |
| Ni                             | 0.23  | 0.62  | -0.50            | 0.30                           | -0.42                          | 0.17              | -0.18            | 0.14                          | 0.28             | 0.46  | 0.19            | 0.83  | 0.08  | 0.62    | 0.93  | 0.73  | 0.94  | 0.86  | 1.00  |       |       |      |       |
| Cu                             | 0.09  | 0.44  | -0.38            | 0.46                           | -0.40                          | 0.04              | -0.14            | 0.26                          | 0.33             | 0.53  | 0.11            | 0.81  | 0.21  | 0.44    | 0.95  | 0.60  | 0.82  | 0.87  | 0.94  | 1.00  |       |      |       |
| Zn                             | 0.01  | 0.09  | 0.20             | 0.88                           | -0.47                          | 0.30              | -0.20            | 0.43                          | 0.02             | 0.50  | -0.46           | 0.49  | 0.07  | 0.09    | 0.53  | 0.12  | 0.30  | 0.71  | 0.51  | 0.66  | 1.00  |      |       |
| Mo                             | 0.39  | 0.36  | -0.36            | 0.42                           | -0.47                          | 0.29              | -0.22            | -0.05                         | -0.06            | 0.45  | 0.13            | 0.61  | -0.18 | 0.36    | 0.85  | 0.47  | 0.90  | 0.82  | 0.93  | 0.87  | 0.59  | 1.00 |       |
| Zr                             | 0.01  | 0.43  | -0.29            | 0.05                           | -0.04                          | 0.11              | -0.03            | 0.03                          | 0.14             | 0.18  | 0.52            | 0.69  | 0.22  | 0.43    | 0.82  | 0.51  | 0.83  | 0.75  | 0.91  | 0.89  | 0.38  | 0.83 | 1.00  |
| Pb                             | 0.25  | 0.67  | -0.49            | 0.23                           | -0.39                          | 0.19              | -0.32            | 0.06                          | 0.28             | 0.47  | 0.26            | 0.87  | 0.20  | 0.67    | 0.88  | 0.72  | 0.89  | 0.90  | 0.98  | 0.91  | 0.46  | 0.89 | 0.90  |
| Rb                             | 0.05  | 0.18  | -0.18            | 0.18                           | -0.06                          | 0.09              | 0.10             | 0.00                          | -0.06            | 0.14  | 0.43            | 0.50  | -0.02 | 0.18    | 0.80  | 0.32  | 0.80  | 0.65  | 0.85  | 0.87  | 0.47  | 0.87 | 0.94  |
| Ga                             | 0.37  | 0.59  | -0.65            | 0.20                           | -0.51                          | 0.37              | -0.11            | 0.04                          | 0.16             | 0.37  | 0.11            | 0.62  | -0.34 | 0.59    | 0.81  | 0.68  | 0.96  | 0.65  | 0.87  | 0.70  | 0.28  | 0.87 | 0.68  |
| Se                             | 0.48  | 0.39  | -0.34            | 0.49                           | -0.57                          | 0.29              | -0.55            | -0.13                         | 0.00             | 0.64  | 0.08            | 0.69  | 0.06  | 0.39    | 0.77  | 0.44  | 0.75  | 0.94  | 0.86  | 0.84  | 0.64  | 0.92 | 0.75  |
| Br                             | 0.22  | -0.14 | 0.02             | 0.79                           | -0.49                          | 0.15              | -0.16            | 0.11                          | -0.16            | 0.53  | -0.22           | 0.33  | -0.16 | -0.14   | 0.66  | 0.03  | 0.47  | 0.66  | 0.59  | 0.74  | 0.86  | 0.76 | 0.51  |
| Y                              | 0.45  | 0.35  | -0.23            | 0.61                           | -0.59                          | 0.19              | -0.57            | -0.05                         | 0.02             | 0.69  | -0.05           | 0.69  | 0.16  | 0.35    | 0.73  | 0.40  | 0.64  | 0.95  | 0.81  | 0.84  | 0.75  | 0.86 | 0.69  |
| Nb                             | 0.06  | 0.38  | -0.87            | 0.02                           | -0.38                          | -0.15             | -0.18            | 0.10                          | 0.68             | 0.53  | 0.19            | 0.52  | 0.18  | 0.38    | 0.65  | 0.54  | 0.51  | 0.35  | 0.46  | 0.46  | -0.07 | 0.29 | 0.37  |
| As                             | 0.75  | 0.36  | -0.75            | 0.35                           | -0.77                          | 0.07              | -0.54            | -0.31                         | 0.10             | 0.74  | 0.01            | 0.50  | -0.23 | 0.36    | 0.71  | 0.51  | 0.76  | 0.65  | 0.71  | 0.60  | 0.25  | 0.77 | 0.48  |
| Te                             | -0.06 | 0.34  | -0.10            | 0.61                           | -0.36                          | 0.17              | -0.18            | 0.39                          | 0.27             | 0.50  | -0.05           | 0.77  | 0.31  | 0.34    | 0.82  | 0.42  | 0.61  | 0.88  | 0.81  | 0.93  | 0.85  | 0.77 | 0.77  |
| Sb                             | 0.60  | -0.52 | 0.16             | 0.57                           | -0.53                          | 0.14              | -0.41            | -0.37                         | -0.54            | 0.39  | -0.55           | -0.42 | -0.52 | -0.52   | -0.22 | -0.49 | -0.24 | -0.03 | -0.27 | -0.22 | 0.29  | 0.05 | -0.45 |

**Table 2** Correlation matrix between the studied elements (Continued)

|    | CaO   | MgO   | SiO <sub>2</sub> | Al <sub>2</sub> O <sub>3</sub> | Fe <sub>2</sub> O <sub>3</sub> | Na <sub>2</sub> O | K <sub>2</sub> O | P <sub>2</sub> O <sub>5</sub> | TiO <sub>2</sub> | SrO   | SO <sub>3</sub> | Cl   | LOI   | Norm.D. | V    | Cr    | Mn    | Co   | Ni   | Cu   | Zn    | Mo   | Zr   |
|----|-------|-------|------------------|--------------------------------|--------------------------------|-------------------|------------------|-------------------------------|------------------|-------|-----------------|------|-------|---------|------|-------|-------|------|------|------|-------|------|------|
| I  | 0.54  | 0.23  | -0.56            | 0.16                           | -0.42                          | -0.03             | -0.51            | -0.43                         | 0.02             | 0.58  | 0.41            | 0.50 | 0.08  | 0.23    | 0.72 | 0.36  | 0.72  | 0.72 | 0.75 | 0.72 | 0.24  | 0.79 | 0.74 |
| Cs | -0.10 | -0.21 | 0.22             | 0.10                           | 0.14                           | -0.05             | -0.48            | -0.24                         | -0.06            | 0.25  | 0.38            | 0.20 | 0.65  | -0.21   | 0.15 | -0.27 | -0.11 | 0.46 | 0.14 | 0.32 | 0.32  | 0.15 | 0.36 |
| Ba | 0.49  | 0.22  | -0.63            | 0.16                           | -0.44                          | -0.08             | -0.44            | -0.36                         | 0.11             | 0.60  | 0.39            | 0.51 | 0.07  | 0.22    | 0.77 | 0.39  | 0.73  | 0.69 | 0.75 | 0.73 | 0.22  | 0.76 | 0.73 |
| La | 0.52  | 0.35  | -0.72            | -0.08                          | -0.37                          | -0.24             | -0.61            | -0.47                         | 0.26             | 0.59  | 0.44            | 0.49 | 0.31  | 0.35    | 0.54 | 0.45  | 0.54  | 0.55 | 0.56 | 0.50 | -0.08 | 0.48 | 0.54 |
| Nd | 0.27  | 0.64  | -0.38            | 0.33                           | -0.49                          | 0.32              | -0.74            | 0.03                          | 0.35             | 0.66  | 0.04            | 0.83 | 0.47  | 0.64    | 0.59 | 0.54  | 0.49  | 0.92 | 0.68 | 0.65 | 0.49  | 0.59 | 0.56 |
| Sm | 0.53  | 0.43  | -0.63            | 0.44                           | -0.68                          | 0.16              | -0.40            | -0.09                         | 0.16             | 0.69  | 0.06            | 0.67 | -0.12 | 0.43    | 0.89 | 0.58  | 0.88  | 0.82 | 0.90 | 0.84 | 0.48  | 0.93 | 0.72 |
| Hf | 0.27  | 0.36  | -0.18            | 0.60                           | -0.52                          | 0.24              | -0.59            | 0.06                          | 0.14             | 0.68  | -0.03           | 0.75 | 0.32  | 0.36    | 0.72 | 0.37  | 0.56  | 0.97 | 0.77 | 0.84 | 0.78  | 0.78 | 0.68 |
| Sc | 0.10  | 0.66  | -0.56            | 0.02                           | -0.21                          | -0.03             | 0.04             | 0.16                          | 0.38             | 0.25  | 0.36            | 0.77 | 0.14  | 0.66    | 0.86 | 0.80  | 0.92  | 0.65 | 0.93 | 0.84 | 0.23  | 0.77 | 0.90 |
| W  | 0.63  | -0.05 | -0.56            | 0.02                           | -0.38                          | -0.16             | -0.57            | -0.67                         | -0.09            | 0.55  | 0.39            | 0.16 | -0.01 | -0.05   | 0.42 | 0.08  | 0.41  | 0.40 | 0.39 | 0.36 | -0.05 | 0.47 | 0.38 |
| Ti | 0.18  | 0.44  | -0.27            | 0.02                           | -0.17                          | 0.41              | 0.32             | 0.12                          | -0.11            | -0.12 | 0.07            | 0.29 | -0.58 | 0.44    | 0.48 | 0.49  | 0.77  | 0.27 | 0.61 | 0.41 | 0.14  | 0.65 | 0.49 |
| Ce | 0.04  | 0.52  | -0.56            | 0.30                           | -0.37                          | 0.03              | -0.21            | 0.23                          | 0.50             | 0.55  | 0.23            | 0.86 | 0.32  | 0.52    | 0.96 | 0.66  | 0.81  | 0.84 | 0.90 | 0.95 | 0.48  | 0.77 | 0.86 |
| U  | 0.32  | 0.52  | -0.46            | 0.26                           | -0.38                          | 0.14              | -0.29            | -0.04                         | 0.15             | 0.47  | 0.30            | 0.77 | 0.12  | 0.52    | 0.89 | 0.61  | 0.90  | 0.88 | 0.98 | 0.93 | 0.48  | 0.94 | 0.93 |
| Th | 0.66  | -0.02 | -0.41            | 0.35                           | -0.50                          | -0.31             | -0.46            | -0.45                         | -0.10            | 0.65  | 0.19            | 0.32 | 0.02  | -0.02   | 0.62 | 0.21  | 0.56  | 0.58 | 0.61 | 0.65 | 0.32  | 0.70 | 0.57 |
| Ta | 0.04  | 0.20  | 0.34             | 0.41                           | -0.11                          | -0.13             | -0.37            | 0.15                          | 0.04             | 0.31  | -0.13           | 0.47 | 0.62  | 0.20    | 0.18 | 0.15  | 0.02  | 0.56 | 0.32 | 0.44 | 0.61  | 0.26 | 0.34 |



**Table 2** Correlation matrix between the studied elements (Continued)

|    | Pb   | Rb   | Ga    | Se   | Br   | Y    | Nb    | As    | Te   | Sb    | I    | Cs    | Ba   | La    | Nd   | Sm   | Hf   | Sc   | W     | Ti    | Ce   | U    | Th   | Ta   |  |
|----|------|------|-------|------|------|------|-------|-------|------|-------|------|-------|------|-------|------|------|------|------|-------|-------|------|------|------|------|--|
| I  | 0.78 | 0.71 | 0.66  | 0.85 | 0.54 | 0.77 | 0.57  | 0.86  | 0.55 | 0.06  | 1.00 |       |      |       |      |      |      |      |       |       |      |      |      |      |  |
| Cs | 0.25 | 0.30 | -0.22 | 0.40 | 0.35 | 0.45 | 0.12  | 0.04  | 0.46 | 0.00  | 0.46 | 1.00  |      |       |      |      |      |      |       |       |      |      |      |      |  |
| Ba | 0.76 | 0.70 | 0.67  | 0.80 | 0.54 | 0.72 | 0.67  | 0.86  | 0.54 | 0.02  | 0.99 | 0.42  | 1.00 |       |      |      |      |      |       |       |      |      |      |      |  |
| La | 0.64 | 0.40 | 0.47  | 0.61 | 0.16 | 0.53 | 0.69  | 0.76  | 0.29 | -0.10 | 0.89 | 0.42  | 0.89 | 1.00  |      |      |      |      |       |       |      |      |      |      |  |
| Nd | 0.79 | 0.37 | 0.50  | 0.82 | 0.37 | 0.81 | 0.41  | 0.59  | 0.68 | -0.07 | 0.65 | 0.50  | 0.61 | 0.63  | 1.00 |      |      |      |       |       |      |      |      |      |  |
| Sm | 0.87 | 0.72 | 0.88  | 0.92 | 0.68 | 0.85 | 0.56  | 0.93  | 0.69 | 0.12  | 0.88 | 0.15  | 0.88 | 0.69  | 0.68 | 1.00 |      |      |       |       |      |      |      |      |  |
| Hf | 0.81 | 0.63 | 0.51  | 0.93 | 0.76 | 0.97 | 0.28  | 0.60  | 0.90 | 0.10  | 0.72 | 0.59  | 0.68 | 0.52  | 0.88 | 0.78 | 1.00 |      |       |       |      |      |      |      |  |
| Sc | 0.90 | 0.80 | 0.79  | 0.64 | 0.33 | 0.58 | 0.48  | 0.56  | 0.64 | -0.54 | 0.64 | 0.00  | 0.65 | 0.54  | 0.49 | 0.74 | 0.52 | 1.00 |       |       |      |      |      |      |  |
| W  | 0.43 | 0.38 | 0.40  | 0.58 | 0.33 | 0.49 | 0.58  | 0.78  | 0.18 | 0.27  | 0.89 | 0.44  | 0.89 | 0.88  | 0.43 | 0.66 | 0.44 | 0.29 | 1.00  |       |      |      |      |      |  |
| Ti | 0.52 | 0.54 | 0.81  | 0.38 | 0.23 | 0.26 | 0.01  | 0.40  | 0.24 | -0.16 | 0.22 | -0.56 | 0.21 | -0.02 | 0.05 | 0.50 | 0.12 | 0.64 | -0.06 | 1.00  |      |      |      |      |  |
| Ce | 0.90 | 0.78 | 0.70  | 0.77 | 0.57 | 0.74 | 0.70  | 0.63  | 0.84 | -0.34 | 0.76 | 0.37  | 0.80 | 0.65  | 0.72 | 0.83 | 0.78 | 0.84 | 0.47  | 0.29  | 1.00 |      |      |      |  |
| U  | 0.98 | 0.88 | 0.81  | 0.92 | 0.61 | 0.86 | 0.43  | 0.74  | 0.79 | -0.20 | 0.85 | 0.29  | 0.83 | 0.66  | 0.72 | 0.91 | 0.82 | 0.89 | 0.53  | 0.52  | 0.89 | 1.00 |      |      |  |
| Th | 0.61 | 0.63 | 0.46  | 0.75 | 0.65 | 0.75 | 0.37  | 0.78  | 0.50 | 0.27  | 0.90 | 0.41  | 0.88 | 0.76  | 0.44 | 0.78 | 0.65 | 0.49 | 0.83  | 0.10  | 0.60 | 0.72 | 1.00 |      |  |
| Ta | 0.39 | 0.27 | -0.12 | 0.44 | 0.38 | 0.61 | -0.32 | -0.04 | 0.60 | -0.07 | 0.16 | 0.52  | 0.08 | 0.09  | 0.50 | 0.15 | 0.63 | 0.22 | -0.10 | -0.18 | 0.28 | 0.37 | 0.29 | 1.00 |  |

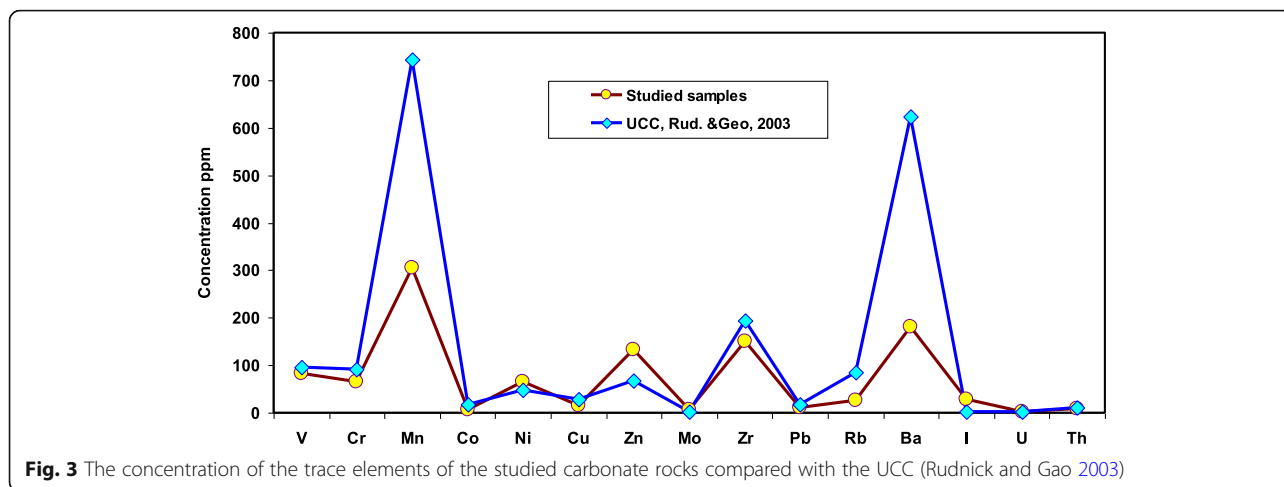


**Fig. 3** The concentration of the trace elements of the studied carbonate rocks compared with the UCC (Rudnick and Gao 2003)

elements of carbonates. Thus, the studied carbonate rocks can be used in cement industries and as building stones (de Silva et al. 2010, Abou El-Anwar et al. 2017 and Abou El-Anwar 2018a).

**Environmental condition**

Al and Mg oxides are important scavengers for trace and REEs, which observed by the positive correlation among them and Al<sub>2</sub>O<sub>3</sub> and MgO. This finding indicates that the distribution of trace and REEs in the studied carbonate rocks is partly controlled by clays and dolomites.

Pi et al. (2014) mentioned that the content of redox-sensitive elements; V, Ni, Mo, U, Cu, Cr, Re, Cd, Sb, Tl, and Mn can be used to indicate paleo-oceanographic environments. The V/Mo and V/(V + Cr) ratios (14.74 and 0.6, respectively) Table 1 indicates that the studied carbonate rocks were deposited in oxic environments (cf. Gallego-Torres et al. 2010; Pi et al. 2014 and Abou El-Anwar 2018a). U/Mo ratio (0.37) indicates the rocks of the studied

area were deposited under an oxic marine transgressive condition (Arning et al. 2009 and Abou El-Anwar 2018b). Depletion of Ce (average = 22.1 ppm) indicated an anoxic environment (De Baar, et al., 1988). Consequently, the studied rocks deposited under anoxic to oxic environment.

The degree of diagenesis can be increased during meteoric and burial diagenesis which was accompanied with loss of U (under oxic conditions), and increase of Zn, Mn, and Fe (Halverson et al. 2007; Webb et al. 2009). Thus, depletion of U and enrichment of Zn and Fe revealed that the deposition of the studied carbonates took place under oxic environment. In addition high content of Sr, Zn, and Ni as trace elements indicated that these carbonate rocks deposited in marine environments.

**Provenance of carbonates**

Some of the elements are used to distinguish between deposits formed in freshwater, shallow-marine, and marine environments, as well as precipitated under surface

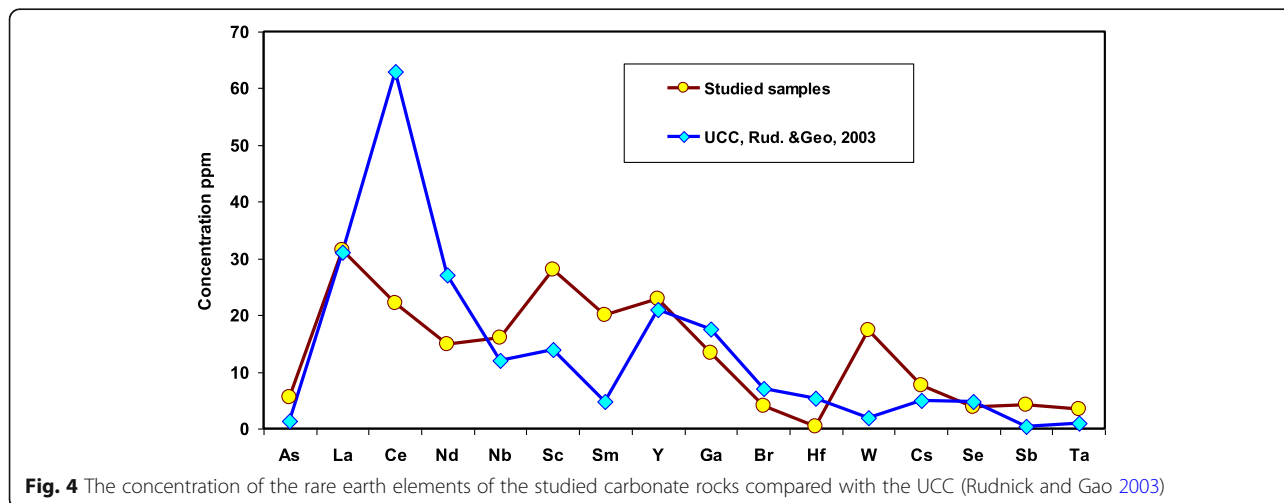
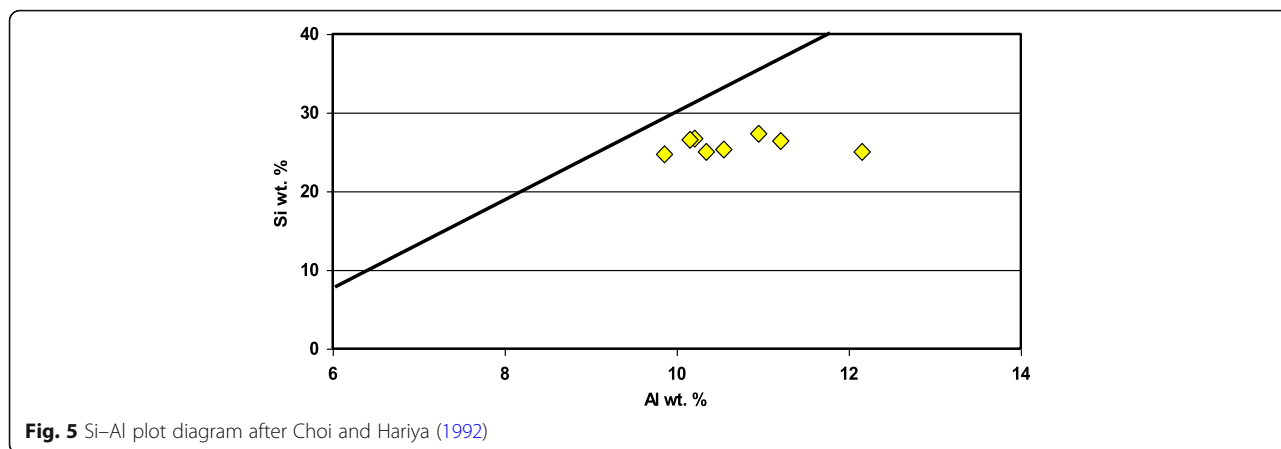


**Fig. 4** The concentration of the rare earth elements of the studied carbonate rocks compared with the UCC (Rudnick and Gao 2003)



or deeper condition. In addition to the rare earth elements, hydrogenous deposits show high  $\Sigma$ REE and those of hydrothermal deposits are considerably lower (Usui and Someya 1997). The studied carbonate rocks show high  $\Sigma$ REE (average of 426 ppm), compared with those of the total in average of continental crust which is about 125 ppm (Rudnick and Gao 2003). Moreover, Si–Al discrimination diagram (Fig. 5) and the (Ni + Co) against (As+Cu+Mo+Pb+V+Zn) as a binary diagram (Fig. 6) according to Choi and Hariya (1992) and Nicholson (1992), respectively, indicated that the studied rocks are mainly hydrogenous sources. Low La/Ce ratios (1.42) and LREE enriched are suggest hydrogenous the origin of the studied carbonate rocks which conformed with Figs. 5 and 6 (Nath et al. 1997).

Trace and rare earth element geochemistry can be used as a tool for sediment provenance (Hu, et al., 2017). The elements such as Cr, Sc, Ta, Th, Zr, Hf, As, and Sb, as well as Y and the rare earth elements (REEs), La to Lu have little mobility in low-temperature, near-surface environments, Thus, they can be useful tool for sediment provenance. Fe and Cr enrichment in pyroxenes and chromite, Sc present in pyroxenes, micas, amphiboles, titanite, and clay minerals, Ti and Ta are found in ilmenite, pyroxene, hornblende, and biotite. Th and

Ta can be hosted in micas, amphiboles, zircon, sphene, and clay minerals; Zr and Hf are associated with zircon, As, and Sb most likely occurring as substitutes for Fe in magnetite; Sc is enriched in pyroxenes; and Th and La are enriched in granitic rocks. As a result, the trace and rare earth elements in the studied carbonate rocks may be derived from more mafic near sources.

The average of LREE enrichment than HREE (~ 102 and 51 ppm, respectively) and the LREE/HREE ratio (2.00) indicated the effect of weathering process on the REE fractionation in the studied carbonate rocks. Thus, the low mobility of LREE than HREE leads to the LREE enrichment, while HREE depletion accompanying with increase weathering effect (Yusoff et al. 2013 and Cao, et al., 2016). Therefore, it is in compatible to the general distribution of REEs in limestone (Gromet et al. 1984; Condie 1991 and Ketris and Yudovich 2009).

The values of the La, Cs, Sc, and Ga indicated that the investigated carbonate rocks were deposited in marine environment (Alibo and Nozaki 1999).

**Conclusions**

The closed correlation between the contents of REE and those of Al, Ca, and Mg is probably due to the vigorous role of calcite, dolomites, and clay minerals in the

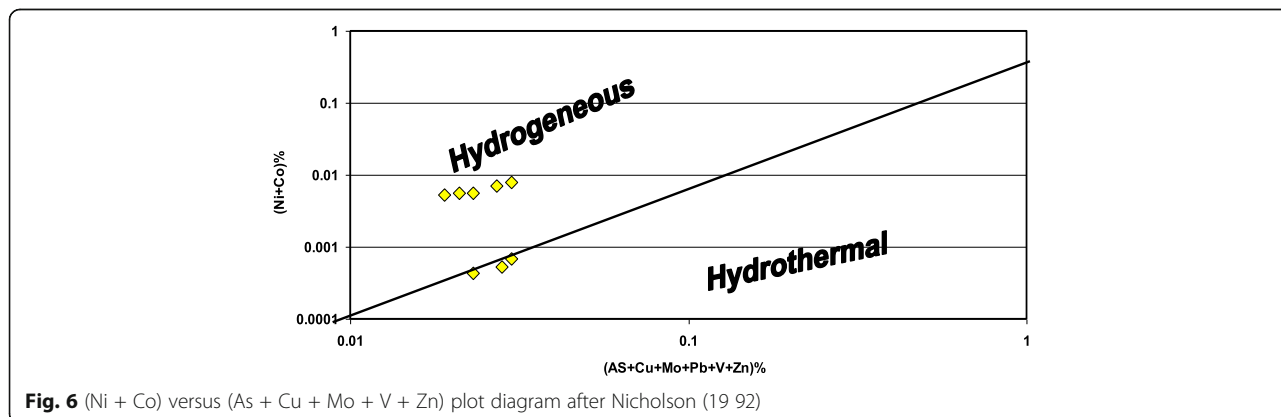


**Fig. 6** (Ni + Co) versus (As + Cu + Mo + V + Zn) plot diagram after Nicholson (19 92)

transfer of REE in the carbonate rocks of Tayiba Formation (Upper Eocene) in Abu Zenima area, West Central Sinai. The studied carbonate rocks deposited under anoxic to oxic marine environments.

The low mobility of LREE than HREE in the studied carbonate rocks leads to the enrichment of LREE than HREE and complementary with increase weathering effect. The high concentration of the ΣREE and plot diagrams are indicated to hydrogenous source of the studied carbonate rocks.

**Acknowledgements**

The author would like to thank the Geological Sciences Dept., National Research Centre, for facilities during this work.

**Author's contribution**

The author read and approved the final manuscript.

**Funding**

No funding

**Availability of data and materials**

All data generated or analyzed during this study are included in this published article.

**Ethics approval and consent to participate**

Not applicable

**Consent for publication**

Not applicable

**Competing interests**

The author declares that there are no competing interests.

Received: 25 September 2019 Accepted: 21 November 2019

Published online: 30 December 2019

**References**

Abou El-Anwar EA (2005) Petrography, geochemistry and genesis of the Upper Eocene carbonate terraces (II and III), Qasr El-Sagha Formation, El-Faiyum, Egypt. *Sedimentology of Egypt* 13:243–260

Abou El-Anwar EA (2006) Petrography, geochemistry and genesis of some Middle Eocene rocks at Qattamia area, Cairo-Suez Road, Egypt. *NRC, Egypt*. 31(6):519–543

Abou El-Anwar EA. Petrographical, geochemical and diagenetic studies of the middle Eocene carbonates Mokattam Formation of Darb El-Faiyum area. In: *Int. Conf. on Geological Sciences and Engineering, Farance, Paris, Augustus 24-26, 2011*; 80: 1315-1325

Abou El-Anwar EA (2014) Composition and origin of the dolostones of Um Bogma formation, Lower Carboniferous, West Central Sinai, Egypt. *Carbonates Evaporates* 29:239–250

Abou El-Anwar EA (2018a) Some carbonate rocks utilized as a building material rocks, Egypt Some carbonate rocks utilized as a building material rocks, Egypt, *Carbonate and Evaporates*, Accepted: 26. <https://doi.org/10.1007/s13146-018-0423-4>

Abou El-Anwar EA. Lithologic characterization of the phosphorite bearing Duwi Formation (Campanian), South Esna, West Nile Valley, Egypt, Accepted: 25 February 2018, on line 2018b, *Carbonates and Evaporites* <https://doi.org/10.1007/s13146-018-0442-1>

Abou El-Anwar EA, Mekky HS, and S. H. Abd El Rahim. Mineralogy, geochemistry, petrography, and depositional environment of Gebel El-Qurn, Early Eocene, West Luxor, South Egypt, *Bulletin of the National Research Centre*, 2018; 42:7, <https://doi.org/10.1186/s42269-018-0008-3>

Abou El-Anwar EA, Mekky HS, Abdel WW (2018) Geochemistry, mineralogy and depositional environment of black, shales of the Duwi Formation, Qusseir area, Red Sea coast, Egypt. *Carbonates and Evaporites*. <https://doi.org/10.1007/s13146-017-0417-7>

Abou El-Anwar EA, Mekky HS, Darweesh HS, Aita SK (2017) Utilization of some Miocene Limestones as building materials from Egyptian north western coastal area (Abu– Sir Ridge). *Carbonates Evaporates*. <https://doi.org/10.1007/s13146-016-0326-1>

Abul-Nasr RAA, Thunell RC (1987) Eocene eustatic sea level changes, evidence from western Sinai, Egypt. *Palaeogeography, Palaeoclimatology, Palaeoecology* 58:1–9

Alibo DS, Nozaki Y (1999) Rare earth elements in seawater: particle association, shale normalization, and Ce oxidation. *Geochim. Cosmochim. Acta* 63(3/4):363–372

Arning ET, Lückge A, Breuer C, Gussone N, Birgel D, Peckmann J (2009) Genesis of phosphorite crusts off Peru. *Mar Geol.* 262:68–81

Brand V, Veizer J (1980) Chemical diagenesis of a multicomponent carbonates systems. 1. Trace elements: *J. Sed. Petrol.* v. 50, p. 1219-1236.

Cao X, Wu P, Cao Z (2016) Element geochemical characteristics of a soil profile developed on dolostone in central Guizhou, southern China: implications for parent materials. *Acta Geochim.* 35(4):445–4

Choi JH, Hariya Y (1992) Geochemistry and depositional environment of Mn Oxide de-posits in the Tokoro Belt, Northeastern Hokkaido. *Econ. Geol* 87:1265–12 74

Choquette PW, James NP (1990) Limestone- the burial diagenetic environment. In: *Diagenesis* (Ed. By I.A. Mcllreath and D.W. Morrow), *Geoscience Canada Reprint Series*, 4

Condie KC (1991) Another look at rare earth elements in shales. *Geochim. Cosmochim. Acta* 55:2527–2531

De Baar HJW, German CR, Elderfield H, Van Gaans P (1988) Rare earth element distributions in anoxic waters of the Cariaco Trench. *Geochim. Cosmochim. Acta* 52,1203–1219

de Silva EF, Ammar M, Celso G, Fernando N, Abdelkrim C, Cristina S, Valdemar E, Ana R, Marques F (2010) Heavy elements in the phosphorite from Kalaat Khasba mine (North-western Tunisia): potential implications on the environment and human health. *J. Hazard. Materials* 182:232–245

El Barkooky AN, El-Araby A (1999) The Tertiary Red Beds of Abu Zenima area, West Central Sinai, Egypt: their stratigraphy and sedimentology. *Proceedings of the Fourth International Conference on the Geology of the Arab World*, pp 621–642

Fedo CM, Eriksson K, Krogstad EJ (1996) Geochemistry of shale from the Archean (~ 3.0 Ga) Buhwa Greenstone belt, Zimbabwe: implications for provenance and source area weathering. *Geochim Cosmochim Acta* 60(10):1751–1763

Gallego-Torres D, Martinez-Ruiz F, De Lange GJ, Jimenez-Espejo FJ, Ortega-Huertas M (2010) Trace-elemental derived paleoceanographic and paleoclimatic conditions for Pleistocene Eastern Mediterranean sapropels. *Palaeogeogr Palaeoclimatol Palaeoecol* 293(1):76–89

Gromet LP, Dymek RF, Haskin LA, Korotev RL (1984) The “North American shale composite”: its compilation, major and trace element characteristics. *Geochim. Cosmochim. Acta* 48:2469–2482

Halverson GP, Dudás FÖ, Maloof AC, Bowring S.A. Evolution of the <sup>87</sup>Sr/<sup>86</sup>Sr composition of neoproterozoic seawater. *Palaeogeogr. Palaeoclimatol. Palaeoecol.*, 2007; 256 (3–4): 103-129

Hu J, Wang H, Wang M (2017) Provenance and tectonic setting of siliciclastic rocks associated with the Neoproterozoic Dahongliutan BIF: implications for the Precambrian crustal evolution of the Western Kunlun orogenic belt, NW China. *J.Asian Earth Sci.* 147, 95–115

Hume W, Madgwick T, Moon F, Sadek H (1920) Preliminary geologic report on Gabal Tanka area. *Petroleum Research Bulletin* 4. Cairo.

Ibrahim AM, Abou El Ezz AR, Mousa AS, El Hariri TYMA, El Ghany A (2016) A.A. Mineralogical and geochemical studies of Eocene Carbonate rocks at Wadi Tayiba and Wadi Feiran areas, Southwestern Sinai, Egypt. *International J. Scient. Engin. Appl. Sci* 2(2):279–304

Jackson CAL, Gawthorpe RL, Leppard CW, Sharp IR (2006) Rift-initiation development of normal fault blocks: insights from the Hammam Faraun fault block, Suez Rift, Egypt. *Journal of the Geological Society of London* 163:165–183

Kamber BS, Webb GE, Gallagher M (2014) The rare earth element signal in Archean microbial carbonate: information on ocean redox and biogenicity. *J. Geol. Soc. Lond.* 171, 745–76

Ketris MP, Yudovich YE (2009) Estimations of clarkes for carbonaceous biolithes: world average for trace element contents in black shales and coals. *Int. J. Coal Geol.* 78:135–148

Loukina SM, Abou El-Anwar EA (1994) Geochemistry of Gebel Ataqa dolostones. *Egypt. Geol. of Egypt* 38:141–156

Loukina SM, Sameeh S, Abou El-Anwar EA (2001) Petrographical and geochemical characteristics of dolostones Of Gaber Formation (Pliocene), Ras Banas, Red Sea Coast, Egypt, *Bull. NRC, Egypt*, v. 26, (4), p. 525-540.

- Moore CH, Chowdhury A (1988) Upper Jurassic Samckover platform dolomitization northwestern Gulf of Mexico: a tale of two waters. In: V. Shukla and P.A. Baker (Eds), *Sedimentology and Geochemistry of Dolostones*, SEPM Special Publ., 43
- Nath BB, Pluger WL, Roelandts I. Geochemical constraints on the hydrothermal origin of ferromanganese incrustations from the Rodriguez triple junction, Indian Ocean. In: Nicholson, K., Hein, J.R., Buh'n, B., Dasgupta, S. (Eds.), *Manganese mineralization: geochemistry and mineralogy of terrestrial and marine deposits*. Geol. Soci. Lond. Spec. Publ, 1997; 119: 199-211.
- Nicholson K (1992) Contrasting mineralogical-geochemical signatures of manganese oxides: guides to metallogenesis. *Econ. Geol* 87:1253–12 64
- Pi DH, Jiang SY, Luo L, Yang JH, Hong-Fei Ling HF (2014) Depositional environments for stratiform witherite deposits in the Lower Cambrian black shale sequence of the Yangtze platform, southern Qinling region, SW China: evidence from redox-sensitive trace element geochemistry. *Palaeogeogr Palaeoclimatol Palaeoecol* 398:125–131
- Refaat AA, Imam MM (1999) The Tayiba Red Beds: transitional marine-continental deposits in the precursor Suez Rift, Sinai, Egypt. *Journal of African Earth Sciences* 26(3):467–506
- Rudnick RL, Gao S (2003) Composition of the continental crust. *Treatise Geochem* 3:1–64
- Tucker ME, Wright VP (1990) *Carbonate sedimentology*. Blackwell Scientific Publ. Oxford 482
- Usui A, Someya M (1997) Distribution and composition of marine hydrogenetic and hydrothermal manganese deposits in the northwest Pacific. In: Nicholson K, Hein JR, Buhn B, Dasgupta S (eds) *Manganese mineralization: geochemistry and mineralogy of terrestrial and marine deposits*, Geol. Soci. Lond. Spec. Publ., vol 119, pp 177–198
- Van Wagoner JC, Posamentier HW, Mitchum Jr, Vail PR, Sarg JF, Loutit TS, Hardenbol J. An overview of the fundamentals of sequence stratigraphy and key definitions. In: Wilgus, C.K., Hastings, B.S., Kendall, C.G.St.C., Posamentier, H.W., Ross, C.A., Van Wagoner, J.C. (Eds.), *Sea level changes: an integrated approach*. Society of Economic Paleontologists and Mineralogists (SEPM) Special Publication, 1988; 42: 39-46.
- Veizer J, Lemieux J, Jones B, Gibling MR, Savelle J (1978) Paleosalinity and dolomitization of a lower paleozoic carbonate sequen. *Can. J. Earth Sci.*, 15, 1448–1461
- Veizer J, Mackenzie FT. Evolution of sedimentary rocks. In: Holland, H.D., Turekian, K.K. (Eds), *Treatise on geochemistry*, 2nd ed. In: Mackenzie, F.T. (Ed.), *Sediments, diagenesis, and sedimentary rocks*, Elsevier-Pergamon, Oxford, 2014; 9: 399-435.
- Webb GE, Nothdurft LD, Kamber BS, Kloprogge JT, Zhao JX (2009) Rare earth element geochemistry of scleractinian coral skeleton during meteoric diagenesis: a sequence through neomorphism of aragonite to calcite. *Sedimentology* 56:1433–1463
- Youssef MI, Abdel Malik WM (1969) Micropaleontological zonation of the Tertiary rocks of the Tayiba-Feiran area, West- Central Sinai, Egypt. *Proceeding of 6th Arab Science Congress, Damascus*:675–684
- Yusoff ZM, Ngwenya BT, Parsons I (2013) Mobility and fractionation of REEs during deep weathering of geochemically contrasting granites in a tropical setting. *Malaysia. Chem. Geol.* 349:71–86

## Publisher's Note

Springer Nature remains neutral with regard to jurisdictional claims in published maps and institutional affiliations.

Submit your manuscript to a SpringerOpen<sup>®</sup> journal and benefit from:

- Convenient online submission
- Rigorous peer review
- Open access: articles freely available online
- High visibility within the field
- Retaining the copyright to your article

---

Submit your next manuscript at ► [springeropen.com](https://www.springeropen.com)

---